

Content Augmented Graph Neural Networks

Fatemeh Gholamzadeh Nasrabadi^{*1}, AmirHossein Kashani^{†1},
Pegah Zahedi^{‡1}, and Mostafa Haghiri Chehreghani^{§1}

¹*Department of Computer Engineering, Amirkabir University of Technology (Tehran Polytechnic), Tehran, Iran*

Abstract

In recent years, graph neural networks (GNNs) have become a popular tool for solving various problems over graphs. In these models, the link structure of the graph is typically exploited and nodes' embeddings are iteratively updated based on adjacent nodes. Nodes' contents are used solely in the form of feature vectors, served as nodes' first-layer embeddings. However, the filters or convolutions, applied during iterations/layers to these initial embeddings lead to their impact diminish and contribute insignificantly to the final embeddings. In order to address this issue, in this paper we propose augmenting nodes' embeddings by embeddings generated from their content, at higher GNN layers. More precisely, we propose models wherein a *structural* embedding using a GNN and a *content* embedding are computed for each node. These two are combined using a combination layer to form the embedding of a node at a given layer. We suggest methods such as using an auto-encoder or building a content graph, to generate *content* embeddings. In the end, by conducting experiments over several real-world datasets, we demonstrate the high accuracy and performance of our models.

Keywords— Graphs (networks), graph neural networks, node embedding (representation), content embedding, structural embedding

1 Introduction

Graphs are an important tool to model data and their relationships. They are used in many domains and applications such as social networks, scientific networks, and protein-protein interaction networks. Several data analysis and machine learning tasks and problems, including classification, regression, clustering and link prediction, have been studied for nodes of a graph or for a collection of graphs. The state of the art recent algorithms for solving these problems rely on computing embeddings (representations) for nodes or graphs. In the embedding (representation) learning task, each node or each graph is mapped to a low-dimensional vector space, so that nodes or

^{*}f.gholamzadeh@aut.ac.ir

[†]amkkashani@aut.ac.ir

[‡]pegahzahedi97@gmail.com

[§]mostafa.chehreghani@aut.ac.ir (corresponding author)

graphs that are similar to each other in the graph space, should find similar embeddings in the vector space. Graph neural networks (GNNs) provide a powerful and popular tool to compute embeddings.

A variety of graph neural networks have been proposed in the literature to generate high-quality embeddings that can enhance the performance of different tasks. They mostly rely on the link structure of the graph and iteratively update the embedding of a node according to its own embedding and the embeddings of its neighbors in the previous iteration (layer). As a result, the local neighborhood of a node plays a critical role in its computed final embedding. However, nodes of a graph usually contain a rich content that can be used to improve several tasks such as node classification and clustering. Existing GNNs mostly use this content only in the form of feature vectors that are fed into them, as nodes' first-layer embeddings. However, consecutive filters (convolutions) that are applied during various iterations/layers, reduce the impact of nodes' feature vectors, so that they find little influence on nodes' final embeddings. As a result, the discriminative power of nodes' content information, which can be useful in many applications, is mostly ignored.

Motivated by this observation and in order to preserve the impact of nodes' contents at higher GNN layers, in this paper we propose novel methods that augment nodes' embeddings with *nodes' content information*, at higher GNN layers. More precisely, we propose a model wherein a *structural* embedding using a GNN and a *content* embedding are computed for each node. These two are combined using a combination layer to form the final embedding of a node at a given layer. We propose two methods to generate *content* embeddings of nodes. In the first method, we build it using an auto-encoder applied to nodes' initial feature vectors to improve them. In the second method, we construct it by forming a content-similarity graph and applying a GNN to this content graph to obtain nodes' *content* embeddings. Our content augmentation methods are independent of the used GNN model and can be aligned with any of them. In this paper, we apply them to three well-known graph neural networks: GCN [12], GAT [20] and GATv2 [4]. Through experiments on several real-world datasets, we demonstrate that our content augmentation techniques considerably improve the performance of GNNs. Furthermore, they outperform several state-of-the-art graph augmentation methods, such as LinkX [14] and skip-connection [23].

The rest of this paper is organized as follows. In Section 2, we provide an overview on related work. In Section 3, we present preliminaries and definitions used in the paper. In Section 4, we present our methods for augmenting graph neural networks with nodes' content information. We empirically evaluate the performance of our proposed methods in Section 5. Finally, the paper is concluded in Section 6.

2 Related work

In this section, we provide an overview of foundational GNN models and recent innovations aimed at enhancing their performance, particularly in the context of preserving and augmenting node features. We discuss seminal models such as Graph Convolutional Networks (GCNs), Graph Attention Networks (GATs), and their improved variant GATv2. Additionally, we explore methods to mitigate common challenges in GNNs, such as over-smoothing, through techniques like skip-connections and the LinkX model. Finally, we highlight the integration of structural and content-based features in GNNs, demonstrating their application in diverse domains.

2.1 GNN models

Graph neural networks (GNNs) are designed to handle graph-structured data by iteratively updating node representations based on their neighbors. The fundamental idea is to aggregate information from a node’s local neighborhood to compute its embedding. In this section, we discuss widely-used GNN models.

Kipf and Welling [12] introduced graph convolutional networks (GCNs), utilizing a spectral-based approach to define convolution operations on graphs. The message-passing mechanism in GCNs can be described as follows: node features are aggregated from neighboring nodes using a normalized adjacency matrix with added self-loops. This normalization aids in maintaining numerical stability and enhances the propagation of information through the network layers. The propagation rule can be defined as:

$$H^{(l+1)} = \sigma \left(\tilde{D}^{-1/2} \tilde{A} \tilde{D}^{-1/2} H^{(l)} W^{(l)} \right),$$

where $\tilde{A} = A + I$ is the adjacency matrix with added self-loops, \tilde{D} is the degree matrix of \tilde{A} , $H^{(l)}$ is the feature matrix at layer l , $W^{(l)}$ is the layer-specific trainable weight matrix, and σ is an activation function.

Velickovic et al. [20] introduced graph attention networks (GATs), which employ an attention mechanism to assign varying weights to different nodes in the neighborhood. This attention mechanism enables the model to focus on the most relevant parts of the graph. In GATs, attention coefficients are calculated for each edge, and these coefficients are used to weigh the node features from neighboring nodes during aggregation. The attention coefficient $\alpha_{vu}^{(l)}$ between nodes v and u at layer l is defined as:

$$e_{vu}^{(l)} = \text{LeakyReLU} \left(a^T \left[W h_v^{(l)} \parallel W h_u^{(l)} \right] \right),$$

where a is a learnable weight vector, W is a shared weight matrix, \parallel denotes concatenation, and $h_v^{(l)}$, $h_u^{(l)}$ are the feature vectors of nodes v and u at layer l . The normalized attention coefficients $\alpha_{vu}^{(l)}$ are then computed using a softmax function:

$$\alpha_{vu}^{(l)} = \frac{\exp \left(e_{vu}^{(l)} \right)}{\sum_{k \in \mathcal{N}(v)} \exp \left(e_{vk}^{(l)} \right)}.$$

The node feature update is then given by:

$$h_v^{(l+1)} = \sigma \left(\sum_{u \in \mathcal{N}(v)} \alpha_{vu}^{(l)} W h_u^{(l)} \right).$$

Brody et al. [4] proposed GATv2, an extension of GAT, which addresses limitations in the original GAT by introducing more expressive attention mechanisms. GATv2 enhances the attention computation process, providing a more flexible and powerful way to aggregate node features based on their importance as determined by the attention mechanism. The attention mechanism in GATv2 is defined as:

$$e_{vu}^{(l)} = a^T \text{LeakyReLU} \left(W \left[h_v^{(l)} \parallel h_u^{(l)} \right] \right),$$

where a is a learnable weight vector and W is a shared weight matrix.

2.2 Mitigating over-smoothing in GNNs

Over-smoothing is a common issue in deep GNNs, wherein node representations become indistinguishable as the number of layers increases. Alon and Yahav [1] studied the challenge of over-squashing in deep graph neural networks, a problem that intensifies with the growing number of GNN layers. They suggested maintaining essential

information flow from the initial layers to a central bottleneck layer. Additionally, they proposed a mechanism to create new edges, connecting crucial nodes to the target node. investigated the use of skip-connections as a simple yet powerful method to address over-smoothing. By creating direct links between non-adjacent layers, skip-connections allow information to bypass certain layers, thus maintaining node-specific features that could be lost in deeper networks. This approach tries to preserve the uniqueness of node representations by ensuring that the initial features are incorporated into the final embeddings. The propagation rule with skip-connections can be described as:

$$H^{(l+1)} = \sigma \left(\tilde{D}^{-1/2} \tilde{A} \tilde{D}^{-1/2} H^{(l)} W^{(l)} \right) + H^{(l)},$$

where the added $H^{(l)}$ term represents the skip-connection from layer l to layer $l + 1$.

One of the works most similar to ours is LinkX. Lim et al. [14] aimed to address the limitations of existing GNNs in non-homophilous graphs by introducing the LinkX method. LinkX separately embeds adjacency and node features and combines them using multilayer perceptrons (MLPs). It employs the following feature update mechanism:

$$H^{(l+1)} = \sigma \left(\tilde{D}^{-1/2} \tilde{A} \tilde{D}^{-1/2} H^{(l)} W^{(l)} \right) + XW^{(0)},$$

where X is the original feature matrix and $W^{(0)}$ is a trainable weight matrix applied to input features. Our approach diverges from LinkX by not only mitigating over-smoothing but also enhancing the discriminative power of node features through content augmentation. While LinkX focuses primarily on preserving the initial node features, our models integrate additional content-based features at higher GNN layers, thereby enriching the node representations with more contextual information. This dual focus on preserving and augmenting node features allows our models to maintain high discriminative power even in deeper GNN architectures.

Recently, several other techniques such as strong transitivity relations [15], balanced Forman curvature [2], positional encodings [5], discrete geometry [2] and central nodes [24] have been employed to augment graph structures and improve the performance of GNNs. Our *content* augmentation methods can be easily aligned with these *structural* augmentation techniques to enhance their effectiveness.

2.3 Fusing structural and content-based features

In recent years, the integration of structural and textual data for different tasks over graphs has gained significant attention. Dileo et al. [8] proposed a temporal graph learning approach that leverages both graph structure and user-generated textual content for dynamic link prediction in online social networks. Their methodology incorporates BERT language models to process textual data and combines it with dynamic GNNs to predict future links. This work is particularly relevant to ours as it highlights the importance of nodes' textual information in predicting link formation.

In recommendation systems, hybrid models that combine GNNs with other representation techniques have shown promise. Spillo et al. [19] introduced a knowledge-aware recommender system (KARS) that integrates GNNs and sentence encoders. Their approach first uses GNNs to learn embeddings from collaborative filtering data and descriptive features. Then, a sentence encoder processes textual content to learn representations. These embeddings are further refined using self-attention and cross-attention mechanisms to predict user preferences. Jin et al. [11] introduced SimP-GCN, a graph convolutional network with the following steps. First, it uses an adaptive technique to fuse structural and node features. Next, it employs a learning approach to predict pairwise feature similarity based on the hidden embeddings of selected node pairs.

In the GIANT model [7], the authors tackled feature scarcity in graph-agnostic contexts by using a pre-trained BERT model to predict neighborhoods from raw textual

data. They extracted feature vectors from the BERT model and seamlessly integrated them into the GNN model. Sawhney et al. [17] proposed a model that integrates deep learning techniques with attention mechanisms to predict stock movements. This model combines financial data, social media text, and inter-company relationships to create a comprehensive prediction tool. It emphasizes the importance of multimodal data and the use of attention mechanisms to capture nuances in stock movement prediction.

3 Preliminaries

We assume that the reader is familiar with basic concepts in graph theory. By $G = (V, E)$, we refer to a graph whose node set is V and edge set is E . By n and m , we respectively denote the number of nodes and the number of edges of the graph. By n_t and m_t we respectively denote the number of training nodes and the number of training edges of the graph. We assume that each node has a feature vector of size d . By $X \in \mathbb{R}^{n \times d}$, we denote the matrix of nodes' feature vectors. By finding vector embeddings for nodes of a graph, we want to encode them as low-dimensional vectors that summarize the structure of the graph. A node embedding function g is a mapping that maps each node in the graph into a low-dimensional vector of real values [9]. The most popular methods to generate vector embeddings are graph neural networks.

At a high level, GNNs consist of the following steps [6]:

- i) for each node v , a neighborhood $N(v)$ is constructed,
- ii) at the first layer, the embedding of node v consists of its features (or e.g., the zero vector, if attributes are absent), and
- iii) at each layer $l + 1$, the embedding of node v is computed using a function f that takes as input the layer- l embedding of v and the layer- l embeddings of the nodes in the neighborhood of v . Function f consists of the following components: i) a linear transformation defined by (at least) one trainable weight matrix W that converts a lower layer embedding into a *message*, ii) an activation function σ , which is element-wise applied to each generated message to induce non-linearity to the model, and iii) an aggregation function *agg* which takes a number of vectors as input, aggregates them, and generates a vector as the higher layer embedding of the node.

As a result, function f is defined as follows:

$$h_v^{(l+1)} = f(v, N(v)) = \text{agg} \left(\sigma \left(W \cdot h_u^{(l)}, \forall u \in N(v) \cup \{v\} \right) \right), \quad (1)$$

where $h_v^{(l+1)}$ and $h_v^{(l)}$ are respectively the vector embeddings of v at layers $l + 1$ and l . A widely used activation function is ReLU, defined as follows: $\text{ReLU}(x) = \max(0, x)$.

4 Content augmented graph neural networks

As already mentioned, our primary concern in this paper lies in the vanishing of essential first-layer information, specifically content information, as it propagates through multi-layer convolutional GNNs. Consequently, the models tend to over-rely on graph structural information during the final decision-making process and pay less attention to nodes' content. In this section, we present two effective models that are designed to augment GNNs with content information. The first model is proper for the supervised setting, wherein enough labeled examples should be accessible during training. This is because of the auto-encoder, utilized within this model: although its encoder/decoder components are inherently unsupervised, in our model, they should be trained with

enough number of examples to learn dimension reduction patterns, effectively. The second model works fine in the semi-supervised setting, wherein a limited amount of labeled data is accessible during training. It constructs a content graph, alongside the input graph, and applies GNN models to both of them. GNNs are known for their superior performance in the semi-supervised setting. As a result, the second model demonstrates outstanding performance in this setting.

In the rest of this section, first, we briefly discuss how the input graph is pre-processed, before feeding it into GNN models. Then we describe our supervised and semi-supervised content augmentation methods. Figure 1 presents a high-level demonstration of content augmentation performed by our proposed models.

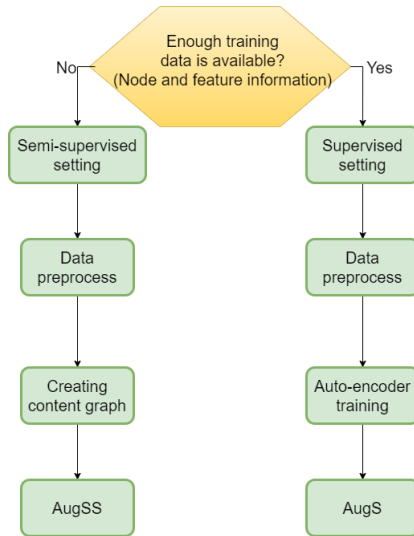


Figure 1: High-level description of content augmentation by our proposed methods.

4.1 Preprocessing

In our data preprocessing phase, we adopt a bag-of-words approach [13] for content processing, creating the initial vectors that will be employed by the GNN layers. The bag-of-words technique represents the content information of the input data, serving as a foundation for subsequent graph-based operations. It should be noted that due to variations in the datasets, this approach results in different first-layer vector sizes. We will elaborate on this in Section 5, providing insights into the impact of diverse dataset characteristics on GNNs’ performance.

Furthermore, to enhance information flow and preserve local content within the graph, it is common practice to augment the graph structure by adding self-loops to each node. Our experiments demonstrate that the addition of self-loops generally improves performance, particularly in the supervised setting where sufficient training data is available. However, an exception to this is the Cora dataset, which features a low average degree and the smallest number of nodes and features. This exception will be discussed further in the experiments section. Adding self-loops does not necessarily lead to performance improvement in the semi-supervised setting (therefore, in the experiments section, we do not report on additional self-loop experiments in the semi-supervised setting).

4.2 Supervised content augmentation of graph neural networks (AugS)

Figure 2 presents the high level structure of our proposed model for content augmentation of graph neural networks, in the supervised setting. This model is compatible with any graph neural network and does not depend on the specific model used. As mentioned earlier, this model is primarily effective in supervised scenarios, as deep auto-encoders tend to have limited functionality in cases of data scarcity. We refer to this supervised content augmentation model as AugS-GNN. In the following, we describe each component of the model in details¹.

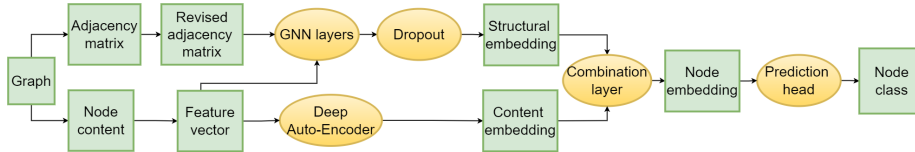


Figure 2: High-level structure of AugS-GNN. Yellow units are computational and green units are data.

4.2.1 Structural and content embeddings

As mentioned earlier, we create two distinct embeddings for each node. First, we utilize the GNN model, which incorporates both the graph structure and features generated from the bag-of-words approach. In this way, a *structural* embedding is built for each node. Then, in order to add a stronger dimension of content information, at higher GNN layers and for each node, we generate a *content* embedding. This is done by feeding the first-layer embedding (the initial feature vector) of each node into an auto-encoder. The output of the encoder component of the auto-encoder serves as the *content* embedding.

For auto-encoder, we use the model based on multiple MLP encoder layers and multiple MLP decoder layers, introduced by Hinton [10]. In the encoder part, each layer’s size is reduced by half compared to the previous layer, while the decoder part follows an opposite pattern, with each layer’s size being doubled relative to the preceding one. The unsupervised loss function used during training is defined by Equation 2, which helps train the model’s parameters:

$$J(\theta) = \sum_{i=0}^{n_t} \|f_{dec} \circ f_{enc}(x_i) - x_i\|_2^2, \quad (2)$$

where Θ is the set of trainable parameters of the encoders and decoders, operator \circ is function composition, f_{enc} and f_{dec} respectively denote the encoder and decoder functions (each consists of several MLP layers) and x_i represents the initial feature vector of node i . The loss function computes the squared L2 norm of the distance vector between the decoder’s composition of the encoder’s output and the original input. Using it, we try to train the auto-encoder parameters in a way that each vector, after encoding and decoding, becomes close to its original form as much as possible. The summation over n_t considers feature vectors of all nodes of the training dataset. After completing the training phase, we use the output of the last encoder (the input of the first decoder), as the *content* embedding. This layer is called the *bottleneck* layer. It is worth highlighting that the parameters of the auto-encoder are

¹Our implementation of AugS is publicly available at: <https://github.com/amkkashani/AugS-GNN>

not jointly learned with the parameters of the entire model, as a separate loss function is used to train them. We set the input dimension based on the number of node features and the bottleneck dimension to 64.

4.2.2 Combination layer

In this layer, we combine the *structural* and *content* embeddings obtained for each node, to form a unique embedding for it. Our combination layer consists of two phases: the fusion phase, wherein the two structural and content embeddings are fused to form a single vector; and the dimension reduction phase, wherein the dimensionality of the vector obtained from the first phase is reduced. For the first phase, we have several fusion functions, including: *concatenation* where the two vectors are concatenated, *sum* where an element-wise sum is applied to the vectors and *max* where an element-wise max is applied to the vectors. Our experiments demonstrate that concatenation consistently outperforms the other fusion methods across different datasets. Therefore in this paper, we specifically highlight the results achieved using the concatenation function.

For the second phase, we incorporate an MLP, whose parameters are trained jointly with the other parameters of the model (unlike the parameters of the auto-encoder used to generate the *content* embedding).

4.2.3 Prediction head

The embeddings generated by AugS-GNN can be used as the input for several downstream tasks and problems such as classification, regression, and sequence labeling. The method used to address these tasks is called the prediction head. Various machine learning techniques, such as SVD, decision trees, and linear regression, can be used in the prediction process. In the experiments of this paper, our focus is to assess the model’s performance in classifying nodes. To do so, we use an MLP, consisting of two dense hidden layers each one with 16 units, as the prediction head. The parameters of the prediction head are jointly learned with the other parameters of the whole model.

We train our model using the cross entropy loss function [18]. For a single training example, it is defined as follows:

$$-\sum_{k=1}^c T_k \log(S_k), \quad (3)$$

where c is the number of classes and T_k and S_k respectively represent the true probability and the estimated probability of belonging the example to class k . The total cross entropy is defined as the sum of cross entropies of all training examples.

We use the following setting to train the model. We set the number of epochs to 200, batch size to 32, dropout ratio to 0.05 (in the MLP of the prediction head, we set it to 0.2), and the number of GNN layers to 2. We use the Adam algorithm as the optimizer and ReLU as the activation function in the hidden layers and softmax in the output layer.

4.2.4 Complexity analysis

As can be seen in Figure 2, our model consists of three parts: the GNN part, the auto-encoder part, and the prediction head.

- Time complexity of the GNN part for L layers of computation is [20]:

$$O\left(\sum_{l=1}^L (m_l d_{l-1} + n_l d_{l-1} d_l)\right),$$

where n_l and m_l are respectively the number of training nodes and the number of training edges, and d_l is the size of embeddings at layer l .

- In the auto-encoder part, due to the symmetric architecture we use, time complexity and the number of parameters of the encoders are the same as those of the decoders. Therefore, we focus only on the encoders. In the encoding part, let d_{input} and d_{bot} be respectively the size of input layer and the bottleneck layer. Since each layer in the encoding part halves the number of features of the previous layer, the depth of the encoder is

$$\left\lceil \log\left(\frac{d_{\text{input}}}{d_{\text{bot}}}\right) \right\rceil + 1.$$

Since this number is small, we consider it a constant. On the other hand, time complexity of a MLP is

$$O\left(\sum_{i=1}^k n_i d_{i-1} d_i\right),$$

where k is the number of layers in the MLP and is a constant, d_{i-1} is the number of input features to layer i , and d_i is the number of output features of layer i . Letting d_{max} be the maximum size that a layer may have, time complexity of the auto-encoder becomes $O(n_t d_{\text{max}}^2)$. Similarly, it can be shown that the number of parameters of the auto-encoder is $O(d_{\text{max}}^2)$.

- Time complexity of the prediction head, which is a MLP, is $O(n_t d_{\text{max}}^2)$.

Therefore, the overall time complexity of our model is:

$$O(m_t d_{\text{max}} + n_t d_{\text{max}}^2). \quad (4)$$

As a result, our supervised content augmentation method does not increase time complexity order of GNN models.

A single GNN layer and a single MLP layer have the same order of parameters, which is $O(d_{\text{max}}^2)$. Moreover, we consider the depths of all the used neural networks constant. Therefore, the parameter complexity of the GNN, the auto-encoder, and the prediction head is $O(d_{\text{max}}^2)$. Thus, the overall parameter complexity of our method is $O(d_{\text{max}}^2)$, which is the same as the parameter complexity of the original GNN models.

4.3 Semi-supervised content augmentation of graph neural networks (AugSS)

In this section, we present our second content augmentation method, specifically tailored to work in a semi-supervised setting. This approach involves the construction of an auxiliary graph based on nodes' content attributes, which is subsequently integrated with the input graph during GNN processing. By adopting this strategy, we infuse the GNN with the influence of nodes' contents, effectively mitigating the issue of content information degradation within the GNNs. We refer to this semi-supervised content augmentation model as AugSS-GNN. Similar to AugS, this approach is compatible with any graph neural network and does not rely on the particular model employed².

²Our implementation of AugSS is publicly available at: <https://github.com/FatemehGholamzadeh/AugSS-GNN>

4.3.1 Content graph construction

Our second approach for content augmentation in GNNs involves the creation of a "content graph", which is fed into the GNN framework. Henceforth, in this paper, we refer to the input graph as the "structural graph", to distinguish it from the content graph. The construction of the content graph is done through the utilization of inherent features within the graph nodes. Here are two steps for building the content graph:

1. We compute pairwise similarities between initial feature vectors of nodes. We can employ diverse metrics suitable for assessing the similarity between two vectors, such as Euclidean distance, dot product, or cosine similarity. In this paper, we employ cosine similarity.
2. If the similarity value of the feature vectors of two nodes exceeds a certain threshold ϵ , we create an edge between the two nodes. It is important to note that the threshold value varies across different datasets. In this study, we employ a grid search methodology to determine the optimal threshold for each dataset.

4.3.2 Model's architecture

Our semi-supervised strategy for integrating the content graph into the training procedure of graph neural networks is illustrated in Figure 3. Apart from the structural graph, we introduce the content graph as an input to the graph neural network. GNNs take a feature matrix of graph nodes as input. Therefore, both the structural and content graphs require an initial feature matrix to be provided as input to the GNN. In our approach, we employ the same feature matrix X as the initial feature matrix, for both the structural graph and the content graph. We examined alternative techniques, such as vectors generated by the DeepWalk algorithm [16], or initializing the feature matrix for the content graph with a set of structural graph features. We will discuss their results in Section 5. Let's denote the structural graph by G and the content graph by G' . All graph neural networks used in this section have two graph convolution layers. It is important to note that each of these graph convolution layers has its own weight parameters, and they do not share the trainable weight parameters.

First, a graph convolution layer, called Conv1, is applied to each of the graphs, considering the adjacency matrix specific to that graph. Suppose that Conv1 maps input vectors with dimension d to output vectors with dimension d' . After applying this layer to G and G' , we will have two output matrices with the same size $n_i \times d'$. In fact, for each node we will have two vectors of dimension d' . At this stage, we combine these two vectors using an aggregation method, which could be, for example, element-wise averaging or summing, or their concatenation, to obtain a vector of dimension $2d'$. Then, we reduce the dimensionality of this vector to obtain a vector of dimension d' , which is used as input to the next layer.

In our experiments, we also employed an alternative aggregation method that led to improved results. We introduced two scalar trainable parameters, w_1 and w_2 , serving as the weights for the structural graph and content graph outputs, respectively. As a result, if we denote the structural graph output with h_1 and the content graph output with h_2 , the combined output can be computed as follows:

$$h = w_1 \times h_1 + w_2 \times h_2. \quad (5)$$

We train these two weights throughout the network's training process, along with the other parameters. This dynamic training approach allows us to adaptively determine the significance of each embedding component.

The second layer of the graph neural network (Conv2), which is also the final layer, takes input vectors of dimension d' and maps them to vectors of dimension c , where c is

the number of classes in node classification tasks. Therefore, by applying the softmax function, the class of each node is determined. Similar to the AugS method, we use cross entropy as the loss function. Figure 3 illustrates our second model’s architecture.

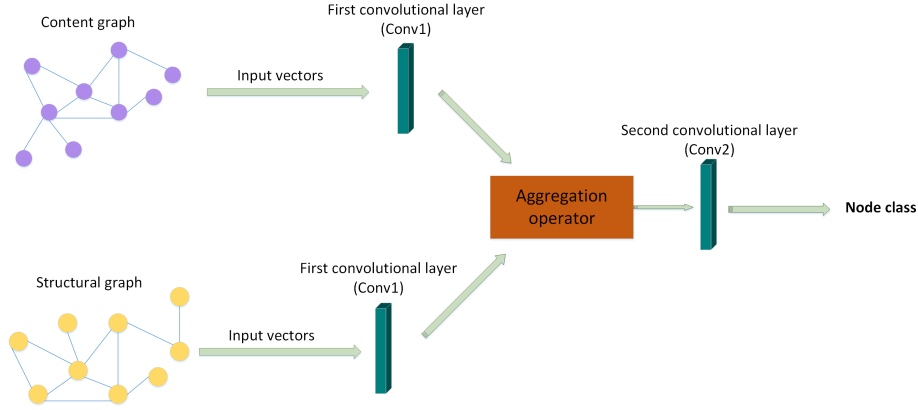


Figure 3: The high-level architecture of AugSS-GNN.

4.3.3 Complexity analysis

AugSS employs two distinct graph convolution layers, applied to both the structural graph G and the content graph G' .

- The first convolution layer transforms input vectors of dimension d to output vectors of dimension d' . Therefore, time complexity of the first convolution layer on both graphs is $O(m_t d_{\max} + n_t d_{\max}^2)$, where d_{\max} is the maximum size that a layer may have.
- The outputs of the first convolution layer for both graphs are aggregated, which incurs an additional complexity of $O(n_t d_{\max})$ for element-wise operations or $O(n_t d_{\max}^2)$ for concatenation and dimensionality reduction.
- The second convolution layer, which maps the aggregated vectors, contributes a complexity of $O(m_t d_{\max} + n_t d_{\max}^2)$.

Thus, the total time complexity of AugSS-GNN is $O(m_t d_{\max} + n_t d_{\max}^2)$, which is equal to that of a standard GNN model. The only computational overhead arises from the preprocessing step to construct the content graph, which involves computing a similarity measure between every pair of nodes, resulting in a complexity of $O(dn_t^2)$. However, these similarities are computed and stored once, eliminating the need for recalculation in subsequent model runs. Furthermore, in inductive settings, when a new node enters the graph, its similarity with other nodes only needs to be computed once, which has a complexity of $O(dn_t)$.

The number of parameters of AugSS-GNN is primarily determined by two graph convolution layers and an aggregation step, each with $O(d_{\max}^2)$ parameters. Therefore, the parameter complexity of AugSS-GNN is $O(d_{\max}^2)$, which is the same as standard GNNs.

5 Experiments

In this section, by conducting experiments over several real-world datasets, we show that our content augmentation techniques considerably improve the performance of GNNs. We choose three well-known GNN models to improve by our augmentation techniques: GCN [12], GAT [20] and GATv2 [4]. Moreover, we compare the augmented GNNs against two well-known GNN augmentation methods, namely LinkX [14] and skip-connection [23]. Furthermore, in order to evaluate the impact of nodes’ features, we compare our methods against an MLP that only exploits nodes’ content information. Additionally, we also consider using embeddings generated by DeepWalk [16] as the input feature vectors for GNNs. The experiments are conducted on a Colab T4 GPU with 16 GB VRAM available for computation.

5.1 Datasets

To evaluate our models, we utilize five widely used datasets: Cora [22], CiteSeer [22], DBLP [3], BlogCatalog [21] and Wiki [21]. The specifications of these real-world datasets are summarized in Table 1. We select these datasets for evaluation due to their inclusion of both graph-based and textual content. We partition each dataset into training, validation, and test sets.

Table 1: Summary of our real-world datasets.

Dataset	#nodes	#edges	Avg. degree	Avg. clustering coefficient	#attributes	#classes
Cora	2708	5278	3.89	0.246175	1433	7
CiteSeer	3312	4732	2.85	0.144651	3703	6
Wiki	2405	17981	14.95	0.323781	4973	17
DBLP	17716	105734	11.92	0.134439	1639	4
BlogCatalog	5196	343486	132.2	0.122371	8189	6

5.2 Evaluation measures

We adopt accuracy, macro-F1 and macro AUC-ROC as the evaluation criteria. Accuracy measures the proportion of correctly classified instances. Macro-F1 accounts for both precision and recall, considering class imbalances and providing a balanced assessment of the model’s performance. They are formally defined as follows.

$$accuracy = \frac{\text{number of correctly classified test examples}}{\text{total number of test examples}} \times 100. \quad (6)$$

$$precision_{class(k)} = \frac{TP_{class(k)}}{TP_{class(k)} + FP_{class(k)}}, \quad (7)$$

where $TP_{class(k)}$ represents the number of correctly predicted examples in class k and $FP_{class(k)}$ indicates the number of examples predicted as class k but belong to other classes.

$$recall_{class(k)} = \frac{TP_{class(k)}}{TP_{class(k)} + FN_{class(k)}}, \quad (8)$$

where $FN_{class(k)}$ is defined as the number of examples in class k that are predicted as belonging to other classes.

$$F1_{class(k)} = \frac{2 \times precision_{class(k)} \times recall_{class(k)}}{precision_{class(k)} + recall_{class(k)}}, \quad (9)$$

and

$$macro-F1 = \frac{1}{c} \times \sum_{k=1}^c F1_{class(k)}, \quad (10)$$

where c is the number of classes.

Macro AUC-ROC provides an aggregate measure of performance across all classes by calculating the Area Under the Curve (AUC) of the Receiver Operating Characteristic (ROC) curve for each class, then averaging these values. The AUC-ROC score represents the probability that a randomly chosen positive instance is ranked higher than a randomly chosen negative instance, with the ROC curve plotting the true positive rate (TPR) against the false positive rate (FPR) at various threshold settings. The AUC-ROC for a single class k is defined as follows:

$$AUC - ROC_{class(k)} = \int_0^1 TPR_{class(k)}(FPR_{class(k)}) dFPR_{class(k)}, \quad (11)$$

where $TPR_{class(k)}$ is the true positive rate for class k and $FPR_{class(k)}$ is the false positive rate for class k . In this formula, TPR is treated as a function of FPR , and FPR serves as the variable of integration. Macro AUC-ROC is then calculated as follows:

$$macro AUC - ROC = \frac{1}{c} \sum_{k=1}^c AUC - ROC_{class(k)}, \quad (12)$$

where c is the number of classes.

5.3 Results

In this section, we present the results of our experiments, in both supervised and semi-supervised settings.

5.3.1 Supervised content augmentation

In the supervised setting, we split each dataset in half for training and testing. We report accuracy, macro-F1 and macro AUC-ROC scores for all the examined methods. We run each model for 10 times and report the average results as well as the standard deviations.

The accuracy results presented in Table 2 show that our augmentation methods usually outperform the other methods. Notably, in specific datasets such as DBLP and BLOGCAT, the enhancements achieved by AugS are considerable. Furthermore, the macro-F1 scores detailed in Table 3 reveal noticeable improvements attributable to AugS, underscoring its effectiveness in handling imbalanced datasets with classes that have few instances. In all the tables, rows marked with * indicate that the model runs with self-loops. To further confirm the high performance of AugS, we report the macro AUC-ROC scores in Table 4.

Table 2: Comparing accuracy scores of the models in the supervised setting.

Model	CORA	CITeseer	WIKI	DBLP	BLOGCAT
GCN	86.92±0.26	73.32±0.08	74.62±0.15	72.85±0.72	70.94±4.25
GCN*	85.39±0.03	76.09±0.08	75.45±0.23	80.21±0.02	71.88±2.97
AugS-GCN	87.41±0.55	72.44±0.38	76.14±0.94	79.46±0.95	85.79±1.8
AugS-GCN*	86.70±0.70	75.78±0.26	75.51±1.12	83.09±0.13	86.04±1.33
GAT	85.11±0.00	75.83±0.13	66.27±1.19	73.25±0.09	59.05±0.41
GAT*	85.27±0.11	77.12±0.11	73.47±0.74	72.83±0.019	64.62±0.50
AugS-GAT	87.65±0.46	74.76±0.52	73.01±1.72	84.58±0.12	67.33±0.68
AugS- GAT *	86.17±0.04	76.34±0.43	73.67±0.60	83.00±0.19	72.52±0.96
GATv2	87.10±0.11	75.90±0.14	72.96±0.58	67.24±0.81	61.78±0.80
GATv2*	86.07±0.03	76.36±0.09	74.44±0.08	79.90±0.62	62.29±0.33
AugS-GATv2	87.52±0.37	75.32±0.16	73.40±1.10	82.18±0.24	68.56±0.62
AugS- GATv2 *	86.01±0.03	74.8±0.22	75.78±0.50	83.69±0.25	70.94±0.81
DeepWalk-GCN	80.56±0.01	62.40±0.12	62.40±0.12	80.73±0.02	63.10±0.12
DeepWalk-GAT	81.27±0.05	62.63±0.06	62.63±0.06	80.49±0.01	61.88±0.05
DeepWalk-GATv2	80.27±0.11	62.82±0.12	62.85±0.12	80.58±0.04	64.57±0.05
MLP	71.8±2.54	69.87±1.52	75.32±1.88	75.76±1.15	85.47±0.50
LinkX	78.87±0.41	58.3±0.45	68.05±0.42	80.04±0.40	72.63±1.21
Skip-connection-GCN	86.51±0.14	72.37±0.10	74.44±0.18	81.54±0.01	85.64±0.03
Skip-connection-GAT	85.90±0.25	72.91±0.28	74.89±0.57	82.48±0.01	77.63±0.50
Skip-connection-GATv2	86.93±0.16	72.41±0.36	73.47±0.31	82.17±0.02	75.26±0.65

Table 3: Comparing macro F1-scores of the models in the supervised setting.

Model	CORA	CITeseer	WIKI	DBLP	BLOGCAT
GCN	84.87±0.12	69.33±0.07	53.72±1.28	61.12±0.39	68.31±7.36
GCN*	83.50±0.03	71.32±0.14	64.00±0.53	64.60±0.06	69.62±4.68
AugS-GCN	86.48±0.50	70.10±0.11	63.89±3.01	60.10±0.23	76.97±0.60
AugS-GCN*	84.19±0.07	69.02±0.63	59.40±3.01	78.73±0.22	85.63±1.34
GAT	82.47±0.03	70.81±0.10	55.03±2.20	50.20±0.054	60.70±4.91
GAT*	83.75±0.14	71.59±0.18	57.17±2.29	54.07±0.13	58.19±0.40
AugS-GAT	86.22±0.65	70.11±0.37	58.79±2.14	77.78±0.41	67.22±0.63
AugS-GAT*	84.52±0.51	71.48±0.79	58.90±3.15	81.34±0.15	71.88±0.98
GATv2	84.87±0.12	69.49±0.10	51.47±2.30	65.47±0.39	61.22±0.87
GATv2*	84.08±0.09	71.50±0.17	57.88±3.12	73.63±0.40	61.615±0.37
AugS-GATv2	85.80±0.62	72.48±0.56	54.58±1.18	77.78±0.41	68.40±0.65
AugS-GATv2*	84.10±0.31	70.22±0.88	58.90±4.16	80.12±0.36	70.57±0.78
DeepWalk-GCN	79.18±0.00	56.38±0.04	42.62±0.06	75.82±0.01	63.40±0.05
DeepWalk-GAT	79.29±0.12	52.07±0.13	42.34±0.03	75.90±0.00	60.35±0.06
DeepWalk-GATv2	79.37±0.08	53.65±0.15	43.20±0.07	75.88±0.07	61.00±0.12
MLP	68.74±3.75	66.89±1.88	66.17±3.80	70.34±2.30	85.25±1.1
LinkX	79.23±0.20	56.80±0.50	68.19±0.39	78.68±1.1	74.2±0.9
Skip-connection-GCN	85.59±0.18	69.01±0.01	63.19±0.13	76.37±0.09	85.04±0.43
Skip-connection-GAT	84.39±0.25	68.85±0.34	64.83±0.68	76.75±0.02	77.57±0.49
Skip-connection-GATv2	85.42±0.17	69.36±0.18	66.16±0.21	75.68±0.04	77.09±0.62

Table 4: Comparing macro AUC-ROC scores of the models in the supervised setting.

Model	CORA	CITeseer	WIKI	DBLP	BLOGCAT
GCN	97.15±0.14	88.17±0.07	92.63±0.01	91.92±0.00	90.95±0.24
GCN*	96.95±0.19	92.50±0.17	92.05±0.01	95.11±0.00	91.65±0.62
AugS-GCN	98.22±0.00	90.12±0.61	94.77±0.00	92.91±0.45	95.96±0.17
AugS-GCN*	97.05±0.01	92.57±0.11	93.40±0.01	95.55±0.56	98.76±0.21
GAT	97.42±0.04	91.66±0.17	87.54±0.97	91.79±0.00	86.45±0.16
GAT*	96.24±0.10	92.48±0.05	88.73±0.08	92.08±0.03	85.47±0.29
AugS-GAT	98.21±0.04	89.56±0.14	88.50±0.07	95.77±0.08	89.56±0.13
AugS-GAT *	96.86±0.05	91.95±0.02	88.98±0.08	95.03±0.12	91.29±0.36
GATv2	97.94±0.01	92.02±0.04	92.41±0.15	89.90±0.33	88.31±0.17
GATv2*	97.09±0.00	92.41±0.01	91.02±0.12	92.38±1.20	86.60±0.42
AugS-GATv2	98.25±0.02	91.98±0.01	93.05±0.07	95.58±0.00	90.92±0.44
AugS-GATv2 *	96.58±0.05	92.11±0.03	94.81±0.21	95.74±0.29	90.86±0.32
DeepWalk-GCN	96.35±0.00	84.57±0.01	88.03±0.00	93.24±0.00	90.53±0.01
DeepWalk-GAT	96.07±0.00	82.56±0.00	88.84±0.00	92.88±0.00	88.40±0.00
DeepWalk-GATv2	96.07±0.00	82.49±0.00	89.33±0.05	93.18±0.00	89.46±0.00
MLP	93.02±0.02	89.75±0.05	92.17±1.77	91.67±0.04	98.52±0.10
LinkX	92.23±0.09	84.7±0.07	85.22±0.15	91.02±0.32	92.51±0.05
Skip-connection-GCN	97.77±0.00	90.61±0.01	94.52±0.06	93.67±0.00	97.3±0.010
Skip-connection-GAT	96.75±0.04	90.37±0.05	94.22±0.15	93.23±0.01	93.72±0.00
Skip-connection-GATv2	97.63±0.01	89.87±0.10	94.48±0.13	93.56±0.00	92.62±0.04

We see in our experiments that having a sufficient number of nodes and features enables supervised methods to rely heavily on node features, particularly when the average degree exceeds 10. Additionally, incorporating self-loops prevents the neural network from losing the initial information of the nodes. Our experiments generally demonstrate that self-loops enhance the performance of the model, except in the Cora dataset, which does not exhibit the same behavior as other datasets. In Cora, we encounter a sparse network with a low number of features, leading to improved performance from the graph structure itself. Therefore, in this case, focusing extra attention on initial features does not enhance the model, resulting in no performance improvement with self-loops in Cora.

AugS, especially in the auto-decoder part, requires substantial training data. Consequently, although it enhances performance in most cases, it exhibits weaknesses over Citeseer, which has a low number of nodes and features, as well as the lowest edge degree among our datasets. On the other hand, over datasets with rich node features and a sufficient number of nodes, such as BlogCatalog, AugS shows significant performance improvements. This weaker performance of AugS over Citeseer is related to the insufficient number of nodes and training data, which negatively impact its functionality.

In order to examine the performance of AugS over different classes, we choose the DBLP dataset and in Figure 4, present the ROC scores of AugS-GAT, across different classes within this dataset. We compare AugS-GAT against four other models: the best skip-connection model (which is skip-connection-GCN), the best DeepWalk model (which is DeepWalk-GCN), MLP, and LinkX. As can be seen, in classes 1 and 2, AugS-GAT and skip-connection-GCN are the best methods. However, in classes 3 and 4, AugS-GAT shows significantly better results than the other methods. It is important to note that although the skip-connection model performs closely to our model over three classes, it does not show a good performance in class 4. This indicates that the skip-connection model may not perform well over minority classes. Conversely, AugS-GAT exhibits high performances across all classes, demonstrating its robustness even in classes 3 and 4, which have a minority population in our dataset.

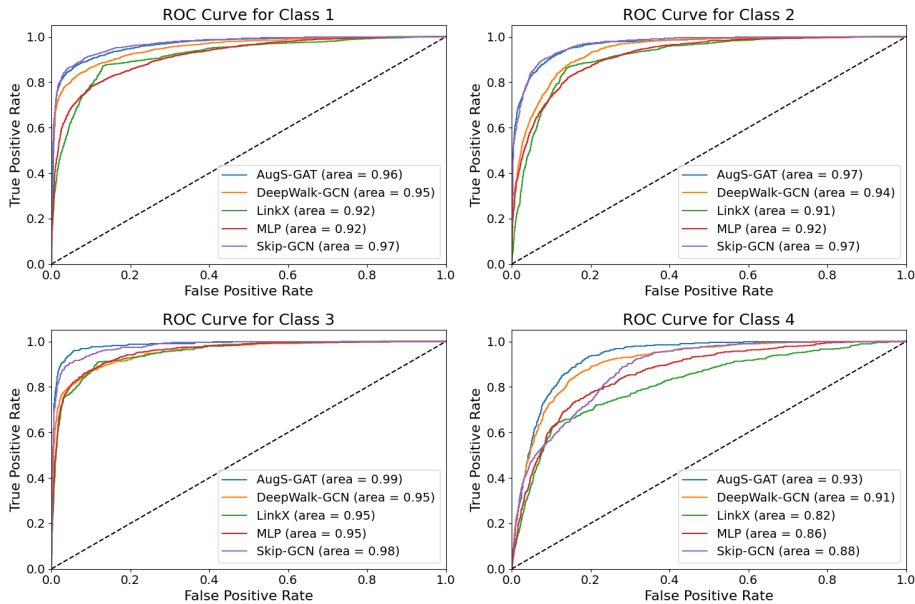


Figure 4: ROC curves of AugS-GAT and the best configurations of the baseline models, in the supervised setting.

Table 5: Class distribution of the DBLP dataset.

class	#examples
1	7920
2	5645
3	1928
4	2169

5.3.2 Semi-supervised content augmentation

In this section, we assess the performance of AugSS-GNN, within a semi-supervised framework. To provide a limited amount of training data for the models, we select 20 labeled samples per class from our datasets and randomly sample 500 data points for validation. Additionally, we allocate 1000 data points for evaluating the models. In the case of the wiki dataset, some classes have fewer than 20 samples, prompting us to select just 5 training samples from these classes. We present accuracy (Table 6), macro-F1 scores (Table 7) and AUC-ROC scores (Table 8), for the examined models. These reported scores are based on the results of 10 runs of the models, where the average accuracy, average macro-F1 and average AUC-ROC as well as the standard deviations are provided in the tables.

Our experiments illustrate the impact of incorporating a content graph into the training process of graph neural networks. By using AugSS, across various datasets, we observe noticeable improvements in the accuracy and F1-scores of the base GNN models, ranging from approximately 2% to 14%. Therefore, AugSS considerably enhances the performance of GNNs, when a limited amount of labeled data is available during the training phase. This improvement in the performance of GNN models is

due to the role of nodes’ content information in their discrimination power, which is better modeled and reflected to the final classifier, using our content augmentation method.

Table 6: Comparing accuracy scores of the models, in the semi-supervised setting.

Model	CORA	CITeseer	WIKI	DBLP	BLOGCAT
GCN	80.81 ± 0.60	69.32 ± 0.69	68.65 ± 1.26	74.92 ± 1.03	75.38 ± 0.83
AugSS-GCN	82.48 ± 0.9	72.85 ± 0.55	72.61 ± 0.84	77.31 ± 0.65	72.87 ± 0.9
GAT	81.17 ± 1.21	68.14 ± 1.51	52.89 ± 3.92	75.4 ± 0.96	63.54 ± 2.5
AugSS-GAT	82.14 ± 0.71	72.46 ± 0.53	59.5 ± 0.74	76.33 ± 0.71	67.6 ± 2.83
GATv2	80.64 ± 0.62	68.2 ± 1.11	50.61 ± 3.31	74.85 ± 1.36	67.57 ± 2.1
AugSS-GATv2	81.62 ± 0.42	72.50 ± 0.69	59.7 ± 1.55	76.42 ± 0.82	81.28 ± 1.33
DeepWalk-GCN	74.50 ± 0.00	45.56 ± 0.19	54.81 ± 0.32	70.44 ± 0.11	60.76 ± 0.05
DeepWalk-GAT	71.26 ± 0.05	42.36 ± 0.18	49.86 ± 0.37	72.74 ± 0.05	56.84 ± 0.05
DeepWalk-GATv2	80.44 ± 0.16	44.44 ± 0.05	52.90 ± 0.12	70.94 ± 0.17	57.00 ± 0.13
MLP	54.32 ± 0.98	58.01 ± 0.83	69.70 ± 0.32	47.93 ± 1.09	68.71 ± 3.96
LinkX	50.45 ± 0.76	36.45 ± 0.37	37.30 ± 0.72	33.31 ± 7.40	57.86 ± 0.47
Skip-connection-GCN	79.30 ± 0.19	65.06 ± 0.13	63.86 ± 0.45	69.10 ± 0.07	78.62 ± 0.23
Skip-connection-GAT	71.24 ± 0.47	65.04 ± 0.61	61.56 ± 0.32	73.12 ± 0.71	40.16 ± 1.06
Skip-connection-GATv2	73.72 ± 0.85	62.60 ± 0.98	60.54 ± 0.32	72.38 ± 1.36	36.34 ± 0.47

Table 7: Comparing F1-scores of the models, in the semi-supervised setting.

Model	CORA	CITeseer	WIKI	DBLP	BLOGCAT
GCN	79.91 ± 0.6	65.62 ± 0.9	58.77 ± 1.6	70.94 ± 0.9	74.70 ± 0.9
AugSS-GCN	81.35 ± 0.9	69.11 ± 0.6	62.78 ± 1.1	74.03 ± 0.8	71.99 ± 1.0
GAT	80.36 ± 1.0	68.45 ± 0.0	43.29 ± 2.9	72.10 ± 0.8	62.99 ± 2.2
AugSS-GAT	81.03 ± 0.9	70.45 ± 2.1	48.85 ± 1.5	72.81 ± 0.8	66.79 ± 2.6
GATv2	79.74 ± 0.6	64.62 ± 0.9	41.60 ± 2.1	71.87 ± 1.3	66.41 ± 2.3
AugSS-GATv2	80.65 ± 0.6	67.78 ± 0.5	47.62 ± 1.7	72.94 ± 1.2	80.74 ± 1.4
Deep walk-GCN	73.61 ± 0.02	42.80 ± 0.18	52.44 ± 0.28	65.57 ± 0.16	58.80 ± 0.06
Deep walk-GAT	70.32 ± 0.02	40.32 ± 0.17	45.45 ± 0.42	67.81 ± 0.07	55.46 ± 0.05
Deep walk-GATv2	78.91 ± 0.19	42.48 ± 0.10	49.05 ± 0.08	66.80 ± 0.18	55.60 ± 0.11
MLP	51.90 ± 1.4	56.52 ± 0.96	69.21 ± 0.45	45.08 ± 1.9	67.77 ± 4.6
LinkX	48.27 ± 1.00	35.60 ± 1.99	35.39 ± 0.24	31.75 ± 7.74	57.88 ± 0.45
Skip-Connection-GCN	78.96 ± 0.18	62.06 ± 0.12	62.18 ± 0.43	66.86 ± 0.07	77.80 ± 0.25
Skip-Connection-GAT	71.99 ± 0.49	61.26 ± 0.56	59.60 ± 0.44	70.59 ± 0.67	39.06 ± 0.92
Skip-Connection-GATv2	73.35 ± 0.65	59.94 ± 0.94	58.99 ± 0.33	69.27 ± 1.49	35.95 ± 0.55

We observe that the improvements in the DBLP and Wiki datasets are more significant compared to the Cora and Citeseer datasets. Additionally, the BlogCatalog dataset shows the greatest improvements among all five datasets. This could be attributed to the average degree of the datasets. The BlogCatalog dataset has a significantly higher average degree, indicating that it is less sparse than the other

Table 8: Comparing macro AUC-ROC scores of the models, in the semi-supervised setting.

Model	CORA	CITeseer	WIKI	DBLP	BLOGCAT
GCN	97.10 \pm 0.33	88.4 \pm 0.01	93.42 \pm 0.0	90.77 \pm 0.06	94.97 \pm 0.14
AugS-GCN	97.24 \pm 0.26	90.66 \pm 0.0	94.8 \pm 0.0	92.04 \pm 0.38	94.97 \pm 0.14
GAT	97.12 \pm 0.21	88.30 \pm 0.48	81.97 \pm 0.04	90.60 \pm 0.05	94.43 \pm 0.09
AugS-GAT	97.26 \pm 0.16	89.34 \pm 0.85	86.55 \pm 0.03	91.65 \pm 0.01	90.59 \pm 0.86
GATv2	96.85 \pm 0.27	88.51 \pm 0.01	87.36 \pm 0.07	91.29 \pm 0.04	91.02 \pm 0.83
AugS-GATv2	96.86 \pm 0.38	90.28 \pm 0.82	89.61 \pm 0.11	92.01 \pm 0.01	95.62 \pm 0.90
DeepWalk-GCN	93.75 \pm 0.00	71.60 \pm 0.03	89.65 \pm 0.01	87.15 \pm 0.02	87.33 \pm 0.01
DeepWalk-GAT	93.65 \pm 0.02	71.25 \pm 0.03	87.67 \pm 0.01	88.41 \pm 0.01	84.58 \pm 0.02
DeepWalk-GATv2	95.05 \pm 0.01	71.03 \pm 0.04	88.88 \pm 0.05	87.85 \pm 0.02	83.10 \pm 0.04
MLP	85.94 \pm 0.02	85.44 \pm 0.06	92.60 \pm 0.03	73.47 \pm 0.03	92.75 \pm 0.11
LinkX	83.21 \pm 0.04	65.28 \pm 1.12	89.46 \pm 0.03	62.26 \pm 1.40	85.96 \pm 0.15
Skip-connection-GCN	96.73 \pm 0.02	87.57 \pm 0.07	93.82 \pm 0.04	90.38 \pm 0.02	94.40 \pm 0.04
Skip-connection-GAT	94.45 \pm 0.07	86.77 \pm 0.21	93.96 \pm 0.05	90.03 \pm 0.07	71.62 \pm 0.55
Skip-connection-GATv2	94.28 \pm 0.17	86.64 \pm 0.06	93.42 \pm 0.11	90.77 \pm 0.32	69.83 \pm 0.47

datasets. This increased connectivity makes it more likely for the effect of initial node features to diminish after several GNN layers. Therefore, incorporating more content information can lead to greater improvements in this case. A similar trend is observed when comparing the Wiki and DBLP datasets with Cora and Citeseer.

To demonstrate the impact of incorporating both content and structural information, we conducted experiments using an MLP that considers only content features as input, and standard GNNs that utilize DeepWalk features, which are structural features, as input. The results, presented in Tables 6, 7 and 8, show that our proposed model, which combines content features with structural features, performs considerably better.

Figure 5 presents the ROC curves of the best configuration of AugSS (which is AugSS-GCN), against the best configurations of the baseline models DeepWalk, skip-connection, MLP, and LinkX, for different classes of the DBLP dataset. As can be seen in the figure, AugSS-GCN consistently outperforms the other models across nearly all classes. The only exception is class 1, where DeepWalk-GAT achieves superior performance. While skip-connection-GATv2 exhibits strong performance in class 3, it does not perform well in other classes. Both LinkX and MLP fail to yield satisfactory results in any of the classes. Moreover, DeepWalk-GAT demonstrates relatively good performance across all classes, particularly in classes 1 and 2, where its results are comparable to those of AugSS-GCN. The poor performance of MLP compared to the good performance of DeepWalk-GAT suggests that structural features are more critical than content features over the DBLP dataset. DeepWalk utilizes only structural features, MLP relies solely on content features, and AugSS-GCN, which combines both structural and content features, outperforms both models.

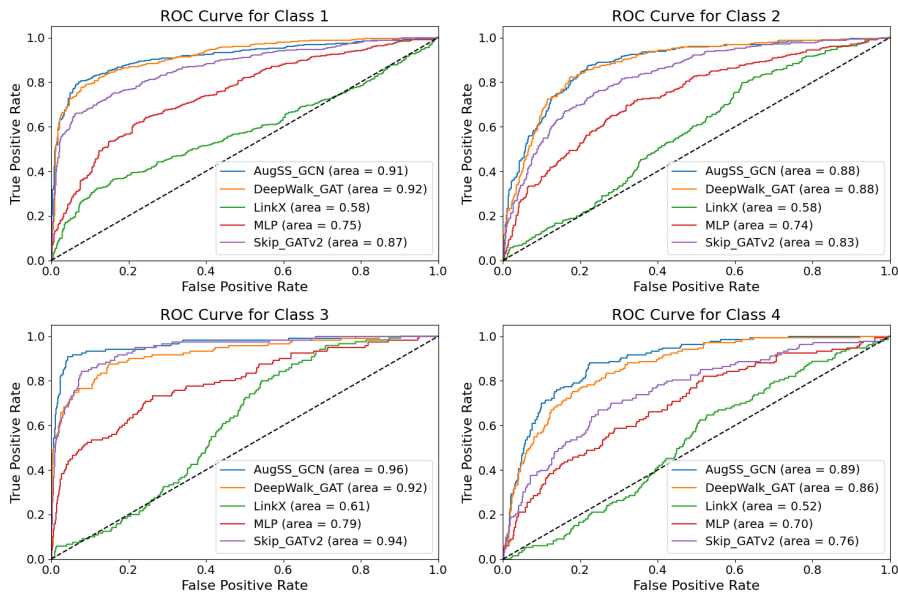


Figure 5: ROC curves of AugSS-GCN against the best configurations of the baseline models, in the semi-supervised setting.

6 Conclusion

In this paper, we proposed novel methods that augment nodes’ embeddings with their content information at higher GNN layers. In our methods, for each node a *structural* embedding and a *content* embedding are computed and combined using a combination layer, to form the embedding of the node at a given layer. We presented techniques such as using an auto-encoder or building a content graph to generate nodes’ *content* embeddings. We conducted experiments over several real-world datasets and showed that our models considerably improve the accuracy of GNN models. In particular, they show high performance when graph nodes have a high number of neighbors, where initial node features are forgotten during the message-passing process.

References

- [1] Uri Alon and Eran Yahav. On the bottleneck of graph neural networks and its practical implications. In *9th International Conference on Learning Representations, ICLR 2021, May 3-7, 2021, Virtual Event, Austria, 2021*. OpenReview.net.
- [2] Jakub Bober, Anthea Monod, Emil Saucan, and Kevin N. Webster. Rewiring networks for graph neural network training using discrete geometry. In Hocine Cherifi, Luis M. Rocha, Chantal Cherifi, and Murat Donduran, editors, *Complex Networks & Their Applications XII*, pages 225–236, Cham, 2024. Springer Nature Switzerland.
- [3] Aleksandar Bojchevski and Stephan Günnemann. Deep gaussian embedding of graphs: Unsupervised inductive learning via ranking. In *6th International Conference on Learning Representations, ICLR 2018, April 30 - May 3, 2018, Conference Track Proceedings, Vancouver, BC, Canada, 2018*. OpenReview.net.

- [4] Shaked Brody, Uri Alon, and Eran Yahav. How attentive are graph attention networks? In *The Tenth International Conference on Learning Representations, ICLR 2022, April 25-29, 2022*, Virtual Event, 2022. OpenReview.net.
- [5] Rickard Brüel-Gabrielsson, Mikhail Yurochkin, and Justin Solomon. Rewiring with positional encodings for graph neural networks, 2023.
- [6] Mostafa Haghiri Chehreghani. Half a decade of graph convolutional networks. *Nature Machine Intelligence*, 4(3):192–193, 2022.
- [7] Eli Chien, Wei-Cheng Chang, Cho-Jui Hsieh, Hsiang-Fu Yu, Jiong Zhang, Olgica Milenkovic, and Inderjit S. Dhillon. Node feature extraction by self-supervised multi-scale neighborhood prediction. In *The Tenth International Conference on Learning Representations, ICLR 2022, April 25-29, 2022*, Virtual Event, 2022. OpenReview.net.
- [8] Manuel Dileo, Matteo Zignani, and Sabrina Gaito. Temporal graph learning for dynamic link prediction with text in online social networks. *Machine Learning*, 113(4):2207–2226, 2024.
- [9] Aditya Grover and Jure Leskovec. node2vec: Scalable feature learning for networks. In Balaji Krishnapuram, Mohak Shah, Alexander J. Smola, Charu C. Aggarwal, Dou Shen, and Rajeev Rastogi, editors, *Proceedings of the 22nd ACM SIGKDD International Conference on Knowledge Discovery and Data Mining, August 13-17, 2016*, pages 855–864, San Francisco, CA, USA, 2016. ACM.
- [10] Geoffrey E Hinton and Ruslan R Salakhutdinov. Reducing the dimensionality of data with neural networks. *science*, 313(5786):504–507, 2006.
- [11] Wei Jin, Tyler Derr, Yiqi Wang, Yao Ma, Zitao Liu, and Jiliang Tang. Node similarity preserving graph convolutional networks. In *14th ACM International Conference on Web Search and Data Mining (WSDM) 2021, March 8-12, 2021*, Jerusalem, Israel, 2021. ACM.
- [12] Thomas N. Kipf and Max Welling. Semi-supervised classification with graph convolutional networks. In *5th International Conference on Learning Representations, ICLR 2017, April 24-26, 2017, Conference Track Proceedings*, Toulon, France, 2017. OpenReview.net.
- [13] Quoc V. Le and Tomás Mikolov. Distributed representations of sentences and documents. In *Proceedings of the 31th International Conference on Machine Learning, ICML 2014, 21-26 June 2014*, volume 32 of *JMLR Workshop and Conference Proceedings*, pages 1188–1196, Beijing, China, 2014. JMLR.org.
- [14] Derek Lim, Felix Hohne, Xiuyu Li, Sijia Linda Huang, Vaishnavi Gupta, Omkar Bhalerao, and Ser Nam Lim. Large scale learning on non-homophilous graphs: New benchmarks and strong simple methods. *Advances in Neural Information Processing Systems*, 34:20887–20902, 2021.
- [15] Yassin Mohamadi and Mostafa Haghiri Chehreghani. Strong transitivity relations and graph neural networks. *CoRR*, abs/2401.01384, 2024.
- [16] Bryan Perozzi, Rami Al-Rfou, and Steven Skiena. Deepwalk: online learning of social representations. In Sofus A. Macskassy, Claudia Perlich, Jure Leskovec, Wei Wang, and Rayid Ghani, editors, *The 20th ACM SIGKDD International Conference on Knowledge Discovery and Data Mining, KDD '14, August 24 - 27, 2014*, pages 701–710, New York, NY, USA, 2014. ACM.
- [17] Ramit Sawhney, Shivam Agarwal, Arnav Wadhwa, and Rajiv Ratn Shah. Deep attentive learning for stock movement prediction from social media text and company correlations. In Bonnie Webber, Trevor Cohn, Yulan He, and Yang Liu, editors, *Proceedings of the 2020 Conference on Empirical Methods in Natural Language Processing, EMNLP 2020, November 16-20, 2020*, pages 8415–8426, Online, 2020. Association for Computational Linguistics.

- [18] Claude Elwood Shannon. A mathematical theory of communication. *The Bell system technical journal*, 27(3):379–423, 1948.
- [19] Giuseppe Spillo, Cataldo Musto, Marco Polignano, Pasquale Lops, Marco de Gemmis, and Giovanni Semeraro. Combining graph neural networks and sentence encoders for knowledge-aware recommendations. In *Proceedings of the 31st ACM Conference on User Modeling, Adaptation and Personalization, UMAP 2023, June 26-29, 2023*, pages 1–12, Limassol, Cyprus, 2023. ACM.
- [20] Petar Velickovic, Guillem Cucurull, Arantxa Casanova, Adriana Romero, Pietro Liò, and Yoshua Bengio. Graph attention networks. In *6th International Conference on Learning Representations, ICLR 2018, April 30 - May 3, 2018, Conference Track Proceedings*, Vancouver, BC, Canada, 2018. OpenReview.net.
- [21] Renchi Yang, Jieming Shi, Xiaokui Xiao, Yin Yang, Juncheng Liu, and Sourav S. Bhowmick. Scaling attributed network embedding to massive graphs. *Proc. VLDB Endow.*, 14(1):37–49, 2020.
- [22] Zhilin Yang, William W. Cohen, and Ruslan Salakhutdinov. Revisiting semi-supervised learning with graph embeddings. In Maria-Florina Balcan and Kilian Q. Weinberger, editors, *Proceedings of the 33rd International Conference on Machine Learning, ICML 2016, June 19-24, 2016*, volume 48 of *JMLR Workshop and Conference Proceedings*, pages 40–48, New York, NY, USA, 2016. JMLR.org.
- [23] Jiaxuan You, Zhitao Ying, and Jure Leskovec. Design space for graph neural networks. *Advances in Neural Information Processing Systems*, 33:17009–17021, 2020.
- [24] Mohammadjavad Zohrabi, Saeed Saravani, and Mostafa Haghiri Chehrehghani. Centrality-based and similarity-based neighborhood extension in graph neural networks. *The Journal of Supercomputing*, 80:1–26, 07 2024.